SECURITY INFORMATION

[redacted]

NACA

RESEARCH MEMORANDUM

for the

Bureau of Aeronautics, Department of the Navy

PRELIMINARY RESULTS OBTAINED FROM FLIGHT TEST OF A $\frac{1}{7}$-SCALE ROCKET-POWERED MODEL OF THE GRUMMAN XF10F AIRPLANE CONFIGURATION IN THE SWEPT-WING CONDITION

TED NO. NACA DE 354

By William N. Gardner

Langley Aeronautical Laboratory
Langley Field, Va.

CLASSIFIED DOCUMENT

This material contains information affecting the National Defense of the United States within the meaning of the espionage laws, Title 18, U.S.C., Secs. 793 and 794, the transmission or revelation of which in any manner to an unauthorized person is prohibited by law.

NATIONAL ADVISORY COMMITTEE FOR AERONAUTICS

WASHINGTON

[redacted]

NACA RM SL52I25

NATIONAL ADVISORY COMMITTEE FOR AERONAUTICS

RESEARCH MEMORANDUM

for the

Bureau of Aeronautics, Department of the Navy

PRELIMINARY RESULTS OBTAINED FROM FLIGHT TEST OF A $\frac{1}{7}$ - SCALE ROCKET-POWERED MODEL OF THE GRUMMAN XF10F AIRPLANE CONFIGURATION IN THE SWEPT-WING CONDITION

TED NO. NACA DE 354

By William N. Gardner

SUMMARY

A flight investigation of a $\frac{1}{7}$ - scale rocket-powered model of the Grumman XF10F airplane in the swept-wing configuration has been made. The purpose of this test was to determine the static longitudinal stability, damping in pitch, and longitudinal control effectiveness of the airplane with the center of gravity at 20 percent of the wing mean aerodynamic chord. Only a small amount of data was obtained from the test because, immediately after booster separation at a Mach number of 0.88, the configuration was directionally unstable and diverged in sideslip. Simultaneous with the sideslip divergence, the model became longitudinally unstable at 3° angle of attack and -6° sideslip and diverged in pitch to a high angle of attack. During the pitch-up the free-floating horizontal tail became unstable at 5° angle of attack and the tail drifted against its positive deflection limit.

INTRODUCTION

At the request of the Bureau of Aeronautics, Department of the Navy, the Pilotless Aircraft Research Division is investigating the aerodynamic characteristics of the Grumman XF10F airplane through the use of rocket-propelled scale models. This paper presents the results obtained from a flight test of a $\frac{1}{7}$ - scale model of the complete airplane in the swept-wing

configuration. The purpose of the present investigation is to determine the static and dynamic longitudinal stability characteristics and the control effectiveness of the Grumman XF10F airplane at transonic speeds. Static directional stability data are also obtained. Reference 1 presents the results obtained from rocket-powered-model flight tests of an XF10F tail-alone configuration.

SYMBOLS

α	angle of attack (with respect to horizontal reference line), deg
β	angle of sideslip, deg
δ	stabilizer deflection, deg
δ_c	servoplane deflection, deg
a_n	corrected normal acceleration per g as obtained from accelerometer
a_l	corrected longitudinal acceleration per g as obtained from accelerometer
a_t	corrected transverse acceleration per g as obtained from accelerometer
g	acceleration of gravity, ft/sec^2
C_N	normal-force coefficient, a_nW/qS
C_Y	side-force coefficient, a_tW/qS
M.A.C.	mean aerodynamic chord, ft
c	chord, ft
W	weight, lb
S	wing area, sq ft
q	dynamic pressure, $\frac{1}{2}\rho V^2$, lb/sq ft
ρ	air density, slugs/cu ft

V	velocity, ft/sec
M	Mach number
t	time, sec
C_{N_α}	rate of change of normal-force coefficient with angle of attack per degree, $\partial C_N/\partial\alpha$
C_{Y_β}	rate of change of side-force coefficient with angle of sideslip per degree, $\partial C_Y/\partial\beta$
C_{h_δ}	rate of change of stabilizer hinge-moment coefficient with stabilizer deflection per degree, $\partial C_h/\partial\delta$
$C_{h_{\dot{\delta}}}$	rate of change of stabilizer hinge-moment coefficient with rate of change of stabilizer deflection, $\frac{\partial C_h}{\partial \frac{d\delta}{dt}}$, sec/deg
I_y	moment of inertia about pitch axis, slug-ft^2
I_z	moment of inertia about yaw principal axis, slug-ft^2
I_x	moment of inertia about roll principal axis, slug-ft^2
I_{xz}	product of inertia with respect to horizontal and vertical axis, slug-ft^2

MODEL AND INSTRUMENTATION

Model

The Grumman XF10F airplane is a turbojet-powered high-speed fighter incorporating a variable-sweep wing mounted high on the fuselage and an all-movable stabilizer mounted on the tip of the swept vertical tail. Drawings of the $\frac{1}{7}$-scale rocket-powered model of the airplane in the swept-wing configuration are shown in figure 1. Photographs of the model are shown in figure 2, and the physical characteristics of the model are listed in table I. The configuration of the model differs from that of the full-scale airplane in that the nose-side air inlets have been faired out to a smooth contour, and the depth of the stabilizer boom has been increased forward of the stabilizer to accommodate

a servomotor. Angle of attack, angle of sideslip, and total-head pressure instruments were added to the configuration as shown in figures 1 and 2.

The all-movable stabilizer is free floating and utilizes an aerodynamic servoplane for positioning. The purpose of this type of horizontal tail is to provide a longitudinal stabilizing and control system which will have satisfactory handling characteristics throughout the speed range up to supersonic speeds without the use of any power boost in the control system. The canard-type servoplane is linked directly to the pilot's control stick. The stabilizer consists of a 53° delta surface with a constant-chord trailing-edge flap linked to the stabilizer in a 1:1 ratio so as to lead the motion of the stabilizer. The canard-type servoplane which is also a 53° delta surface is mounted forward of the stabilizer on a boom. The complete horizontal tail assembly is free floating about a pivot axis located at 29 percent of the stabilizer mean aerodynamic chord. In the present rocket model investigation, a pneumatic piston-type servomotor is located within the tail boom and is used to pulse the servoplane in a square wave manner.

The primary structure of the model is a 7-inch metal torque tube within the fuselage. Heavy fittings are attached to the torque tube and serve as mounting points for the wing and vertical tail. A metal bulkhead is attached to the forward end of the torque tube; and the telemeter unit, as well as part of the pneumatic servo system, is attached to the forward face of this bulkhead. A sheet-metal nose cone covers the telemeter section. The power supply, ballast, and parts of the pneumatic system are attached to the torque tube which contains the modified 6-inch ABL Deacon sustainer rocket motor. The wing consists of a built-up sheet-metal box section with wood tips and leading edge. A machined casting serves as the wing center section and attachment fitting. The vertical and horizontal tails are machined magnesium castings. Laminated wood attached to plywood bulkheads is used as a fuselage fairing to obtain the fuselage contour lines. All the fuselage wood fairing is covered with Fiberglas for added strength.

The first four natural modes of vibration of the wing and vertical tail were measured as well as the torsional stiffness of the wing. These tests showed that the model was less elastic than the full-scale airplane.

During construction of the model after actual weight distribution was known, inertia calculations were made for the model which indicated that the principal axis of inertia was inclined down 7° at the nose. Since it was believed that this inclination was excessive for satisfactory dynamic lateral stability of the model, an analysis of the model dynamic lateral stability was made. The dynamic characteristics of the present rocket model are not similar to the full-scale airplane. The results of

the stability analysis, which was based on estimated aerodynamic derivatives, indicated that, at transonic speeds and high angles of attack, the model could be expected to have neutral lateral stability; consequently, it was decided that lateral instrumentation would be added to the model. Data from these instruments would reveal whether or not lateral oscillations were interfering with the longitudinal data being obtained. This arrangement was considered to be satisfactory since the model would only reach high angles of attack on the peaks of pitch oscillations.

Instrumentation

A standard NACA telemeter unit was included in the model to give information about the following: angle of attack, angle of sideslip, horizontal-tail deflection, servoplane deflection, longitudinal acceleration, normal acceleration, lateral acceleration, and total-head pressure. Angle of attack and angle of sideslip were measured by vane-type instruments mounted on the nose of the model (figs. 1 and 2). The center line of the angle-of-sideslip instrument was parallel to the principal axis of the model. The total-head pressure tube was located on a small strut below the fuselage (figs. 1 and 2). Accelerometers were mounted in the fuselage as close to the center of gravity as possible. CW Doppler radar sets and tracking radar units were used for obtaining data on model velocity and flight path. Atmospheric conditions were determined by radiosonde observations and motion-picture cameras were used to photograph the launching and flight of the model.

TESTS

Figure 3 is a photograph of the model booster combination on the launching platform. The model was boosted to a Mach number of 0.9 by a 6-inch ABL Deacon rocket motor. Approximately 0.7 second after booster burnout the modified ABL Deacon sustainer rocket motor fired and was intended to increase the speed of the model to about $M = 1.4$. The model was flown at the Langley Pilotless Aircraft Research Station at Wallops Island, Va.

The method of conducting the test was to pulse the servoplane in a square wave at an approximate rate of one pulse every $1\frac{1}{2}$ seconds at subsonic speeds and one pulse every second at transonic speeds. The pulse rate was controlled by a pressure-switch actuated governor on the sequence motor. Deflection limits on the servoplane were 1° and -4°. Stops were provided to limit the free-floating horizontal-tail deflection at 2° and -5°. From the transient oscillations of the tail and the complete model

after a pulse of the servoplane, the airplane static stability, damping, and lift-curve slope were to be determined as well as the control effectiveness, hinge moments, trim, and damping of the horizontal tail.

The model was flight tested with the center of gravity located at 20 percent of the wing mean aerodynamic chord and all accelerometer, angle-of-attack, and angle-of-sideslip data were corrected to give values at the center of gravity.

RESULTS AND DISCUSSION

Time History

Figure 4 is a time history of the data obtained from flight tests of the model during the 1-second interval from just before booster rocket burnout to immediately after sustainer motor ignition. During this period of time the model was coasting at an average speed corresponding to a Mach number of 0.88 and a Reynolds number of approximately 10×10^6. As the booster unit started separating from the model, the servoplane received its first pulse from floating position to the 1° deflection and a small oscillation of the horizontal tail resulted. The angle of attack of the model did not change since the booster unit was not free of the model. Until this time both the angle of attack and angle of sideslip were near 0°. Approximately 0.3 second after the servoplane pulse, the horizontal tail received a disturbance of unknown origin. Examination of motion-picture photographs of the flight reveals the possibility that, as the booster separated from the model and the forward end of the booster entered the air stream, a strong pressure disturbance in the tail flow field may have been created. Such a disturbance could have lasted only for a very short time.

Immediately after booster separation a divergence in sideslip occurred while the angle of attack increased slowly to about 3°. The angle of attack then remained reasonably constant until the angle of sideslip reached -6°. At this point the model started a pitch divergence and both the angle of attack and angle of sideslip exceeded the limits of instrumentation. The limit of the angle of sideslip and angle-of-attack indicators was approximately -10° and 15°, respectively. The model was diverging at a rapid rate in both directions at the time the instruments reached their limit. During this time both the lateral and normal accelerometers were following the model motions and reached their limits at 5g and 20g, respectively. The horizontal tail continued to oscillate in a normal manner damping to low amplitude during the sideslip divergence. As the angle of attack reached about 5°, the free-floating horizontal tail became unstable and drifted against its positive stop. The

servoplane deflection remained constant during this time. Shortly after the preceding instruments had reached their stops, the sustainer rocket motor fired, and, throughout the rest of the flight, there were no other intelligible data available from the telemeter records. Motion-picture records of the flight show that the model executed an extremely violent spiral flight path until shortly after sustainer burnout and thereafter was either in a very tight spiral or tail spin until the end of the flight.

Directional Stability

Analysis of these flight results reveals that the model was directionally unstable at low angles of attack. Figure 5 is a plot of the variation of side-force coefficient with angle of sideslip at $M \approx 0.88$ and shows that, at low angles of sideslip, the value of C_{Y_β} is -0.015, whereas at approximately -8° sideslip, $C_{Y_\beta} = -0.020$. The angle of attack in each case was less than 5°. These values of C_{Y_β} are in agreement with estimated values; however, in the previously mentioned dynamic lateral stability analysis, directional instability was not indicated. Low-speed wind-tunnel tests made by the Grumman Aircraft Engineering Corporation and other unpublished low-speed wind-tunnel tests indicate a value of approximately 0.001 for C_{n_β}. Unpublished high-speed wind-tunnel tests, made since the flight test of the subject model, indicate decreasing directional stability at zero angle of attack as Mach number increases. At $M = 0.8$ the tests show neutral directional stability and also show directional instability from $M = 0.8$ to $M = 0.94$. The data from these tests are in agreement with the results obtained from the present rocket model. As noted in figures 1 and 2 the airplane is a high-wing high-tail configuration and the vertical tail overhangs the short stubby fuselage for a large portion of the fin root chord. Reference 2 shows that a high-wing high-tail configuration has less satisfactory directional stability characteristics than a low-wing low-tail configuration. The fact that the vertical tail overhangs the fuselage undoubtedly decreases the fuselage end-plate effect on the vertical tail, thus causing a reduction in vertical tail effectiveness. These facts when considered in conjunction with possible Mach number effects may be responsible for the loss in directional stability of the model. The possible influence on the directional stability characteristics of the configuration of a jet exhaust under the overhanging vertical tail cannot be estimated at this time.

Lift and Longitudinal Stability

Figure 6 is a plot of the variation of normal-force coefficient with angle of attack at $M \approx 0.88$ and shows that, in the angle-of-attack range from 0° to 3°, the value of C_{N_α} is 0.070. At 3° angle of attack the slope of the curve breaks rapidly until at 10° angle of attack the value of $C_{N_\alpha} = 0.019$. This break in the lift-curve slope is in agreement with previous experience; however, the break would have been expected to occur at a slightly higher angle of attack. It should be pointed out that, at the time this break in slope occurred, the angle of sideslip had increased to -6° and continued to increase as the angle of attack increased. During the time that the angle of attack was increasing from 3° to the 15° limit of the instrument, the configuration was longitudinally unstable. There was no evidence of any tendency either to trim out at a high angle of attack or to oscillate. This characteristic is similar to the pitch-up which has been encountered on several high-speed airplanes and was undoubtedly aggravated by the sideslip divergence and resulting large angles of sideslip.

Free-Floating Horizontal Tail

Figure 7 is a plot of the trim horizontal-tail deflection against angle of attack during the time of the pitch divergence at $M \approx 0.88$ and $\delta_c = 1^\circ$. These data represent the floating characteristics of the free-floating stabilizer as the angle of attack of the model changes and indicate that, over the angle-of-attack range from 3° to 5°, the tail is neutrally stable, $\frac{\partial \delta}{\partial \alpha} = 0$. Above 5° angle of attack the tail is unstable. During this time the model is at a high angle of sideslip, β being greater than -10° above 5° angle of attack. Near zero angle of attack the approximate value of $\partial\delta/\partial\alpha$ is -0.1 which is in good agreement with data shown in reference 1. In reference 1, which presents tail-alone configuration data, it is also shown that at subsonic speeds the tail stability (value of $\partial\delta/\partial\alpha$) decreases rapidly as angle of attack is increased and approaches zero at 8° angle of attack. The data from this present test are then in reasonably good agreement with the tail-alone tests since wing downwash and the large angle of sideslip present would be expected to cause some change in the tail stability. The period of the tail deflection oscillation after the tail disturbance is 0.060 second which corresponds to a value of -0.014 for the hinge-moment derivative C_{h_δ}, and the time to damp to half-amplitude is 0.08 second which corresponds to a value of -0.038 for the tail damping derivative $C_{h_{\dot{\delta}}}$. These values are in fair agreement with the data of reference 1.

CONCLUDING REMARKS

Data obtained from flight test of a rocket-powered model of the Grumman XF10F airplane in the swept-wing configuration show that, at a Mach number of 0.88 and center-of-gravity position at 20 percent of the mean aerodynamic chord, the model is directionally unstable at least through the positive angle-of-attack range up to 15° and also longitudinally unstable above 3° angle of attack and -6° angle of sideslip. The loss in longitudinal stability is accompanied by a large decrease in lift-curve slope. The free-floating horizontal tail is unstable above 5° angle of attack.

Langley Aeronautical Laboratory,
National Advisory Committee for Aeronautics,
Langley Field, Va.

William N. Gardner

William N. Gardner
Aeronautical Research Scientist

Approved: Joseph A. Shortal
Joseph A. Shortal
Chief of Pilotless Aircraft Research Division

JLC

REFERENCES

1. Gardner, William N., and Edmondson, James L.: Preliminary Results Obtained From Flight Test of a Rocket Model Having the Tail Only of the Grumman XF10F Airplane Configuration. TED NO. NACA DE 354. NACA RM SL51E04, Bur. Aero., 1951.

2. Goodman, Alex: Effects of Wing Position and Horizontal-Tail Position on the Static Stability Characteristics of Models With Unswept and 45° Sweptback Surfaces With Some Reference to Mutual Interference. NACA TN 2504, 1951.

TABLE I

MODEL PHYSICAL CHARACTERISTICS

Wing:	
Span, ft	5.24
Mean aerodynamic chord, ft	1.76
Area, sq ft	9.18
Aspect ratio	3.0
Taper ratio	0.75
Sweepback of 0.25-chord line, deg	42.5
Dihedral angle, deg	-5
Incidence, deg	0
Airfoil section (parallel to free stream)	NACA 64A(008)009
Vertical tail:	
Span (exposed), ft	1.095
Mean aerodynamic chord (exposed), ft	1.582
Area (exposed), sq ft	1.78
Aspect ratio (exposed)	0.675
Taper ratio (exposed)	0.486
Sweepback of 0.25-chord line	54°26'
Airfoil section (parallel to free stream)	NACA 64A008
Horizontal tail:	
Stabilizer	
Delta surface, deg	53.2
Mean aerodynamic chord, ft	1.14
Area, sq ft	1.47
Aspect ratio	2.0
Airfoil section	GAEC-004 (similar to NACA 0004)
Pivot-point location, percent mean aerodynamic chord	29
Flap linkage ratio	1:1
Servoplane	
Delta surface, deg	53.2
Mean aerodynamic chord, ft	0.329
Area, sq ft	0.122
Aspect ratio	2.0
Airfoil section	GAEC-006 (similar to NACA 0006)

TABLE I.- Concluded

MODEL PHYSICAL CHARACTERISTICS

Model:	
Weight (loaded sustainer rocket), lb	328.5
Center of gravity (loaded sustainer rocket), percent mean aerodynamic chord	20
Pitch inertia, I_Y, slug-ft^2	34.24
Yaw inertia, I_Z, slug-ft^2	35.10
Roll inertia, I_X, slug-ft^2	3.82
Product of inertia, I_{XZ}, slug-ft^2	3.9
Inclination of principal axis, deg	-7
Moment of inertia of horizontal tail about pivot axis, slug-ft^2	0.142

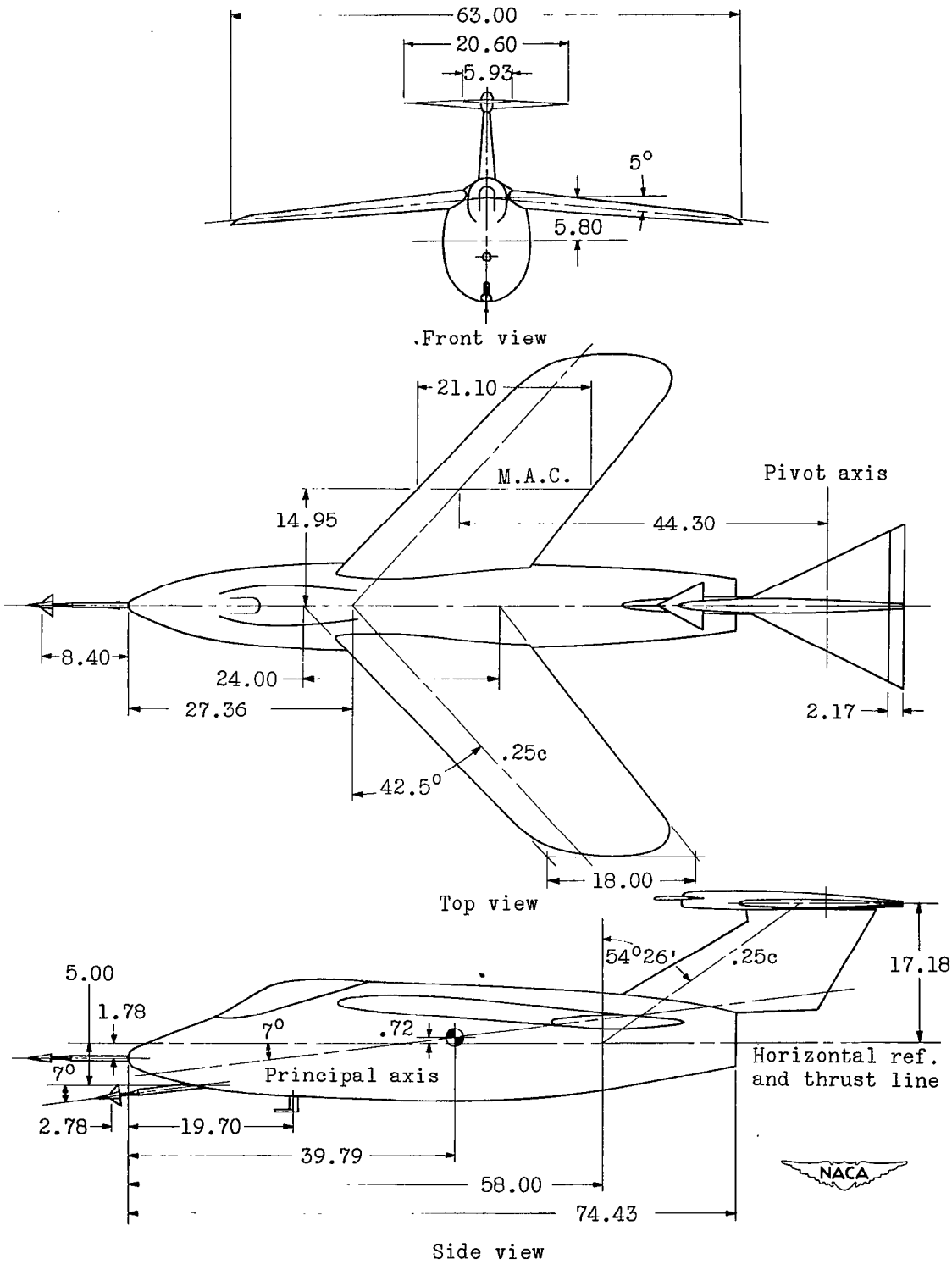

Figure 1.- Three-view drawing of model. All dimensions are in inches.

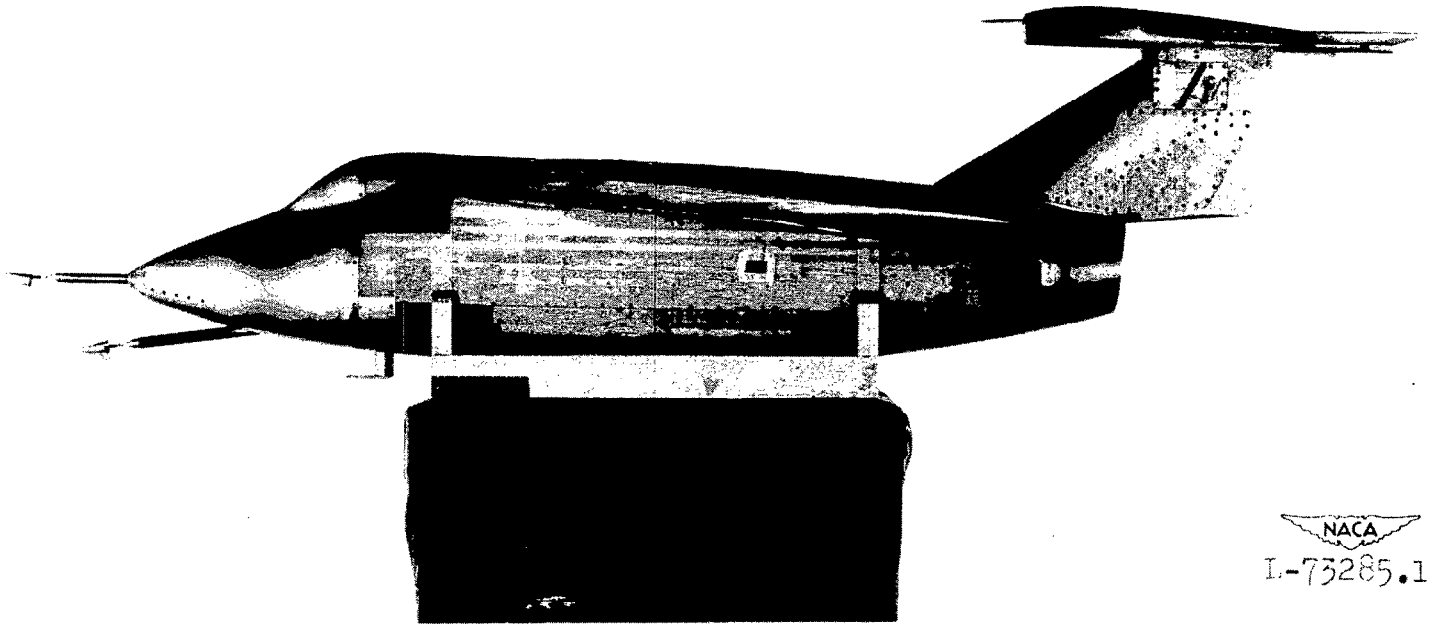

(a) Side view.

Figure 2.- Photographs of model.

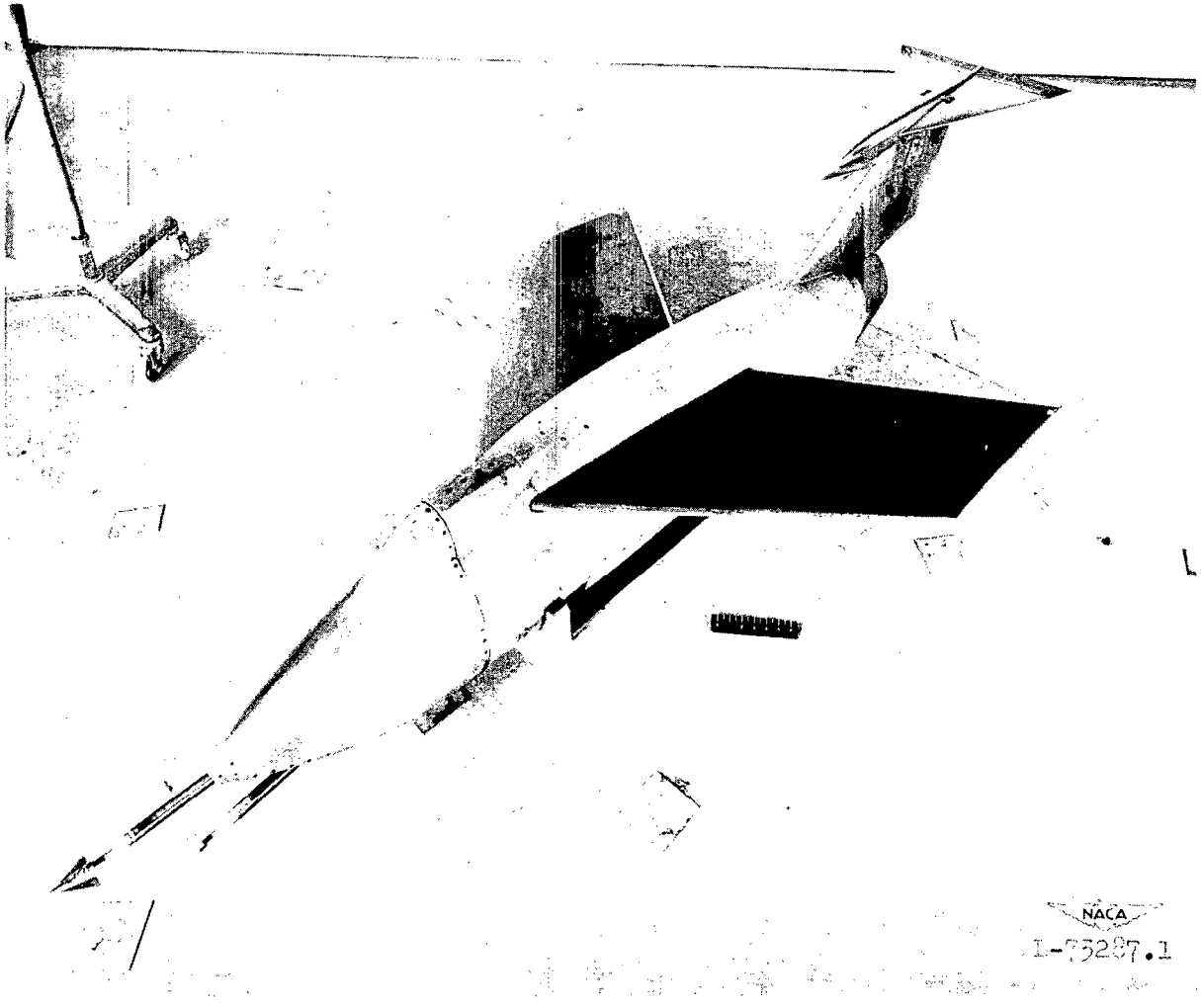

(b) Three-quarter top view.

Figure 2.- Concluded.

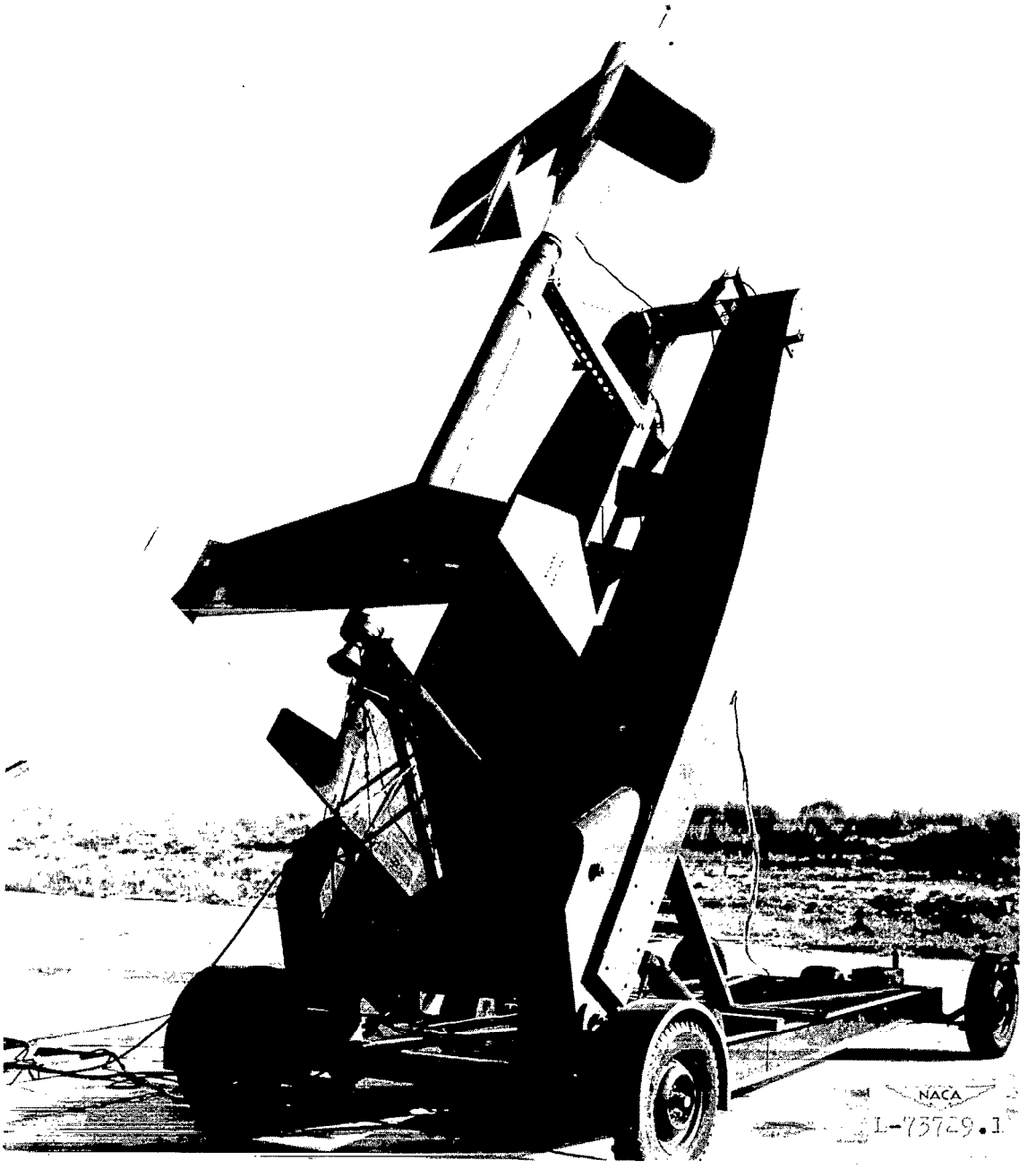

Figure 3.- Model booster combination on launcher.

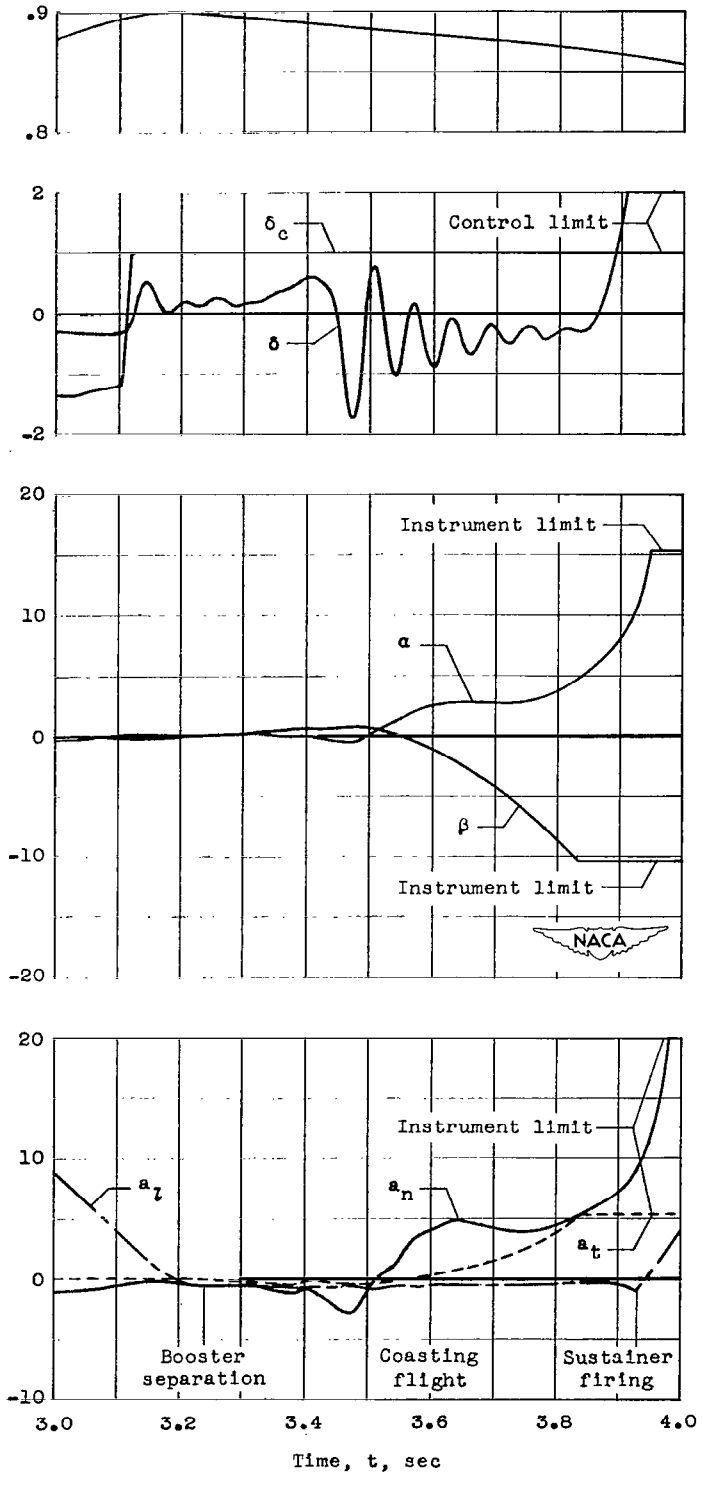

Figure 4.- Time history of flight data.

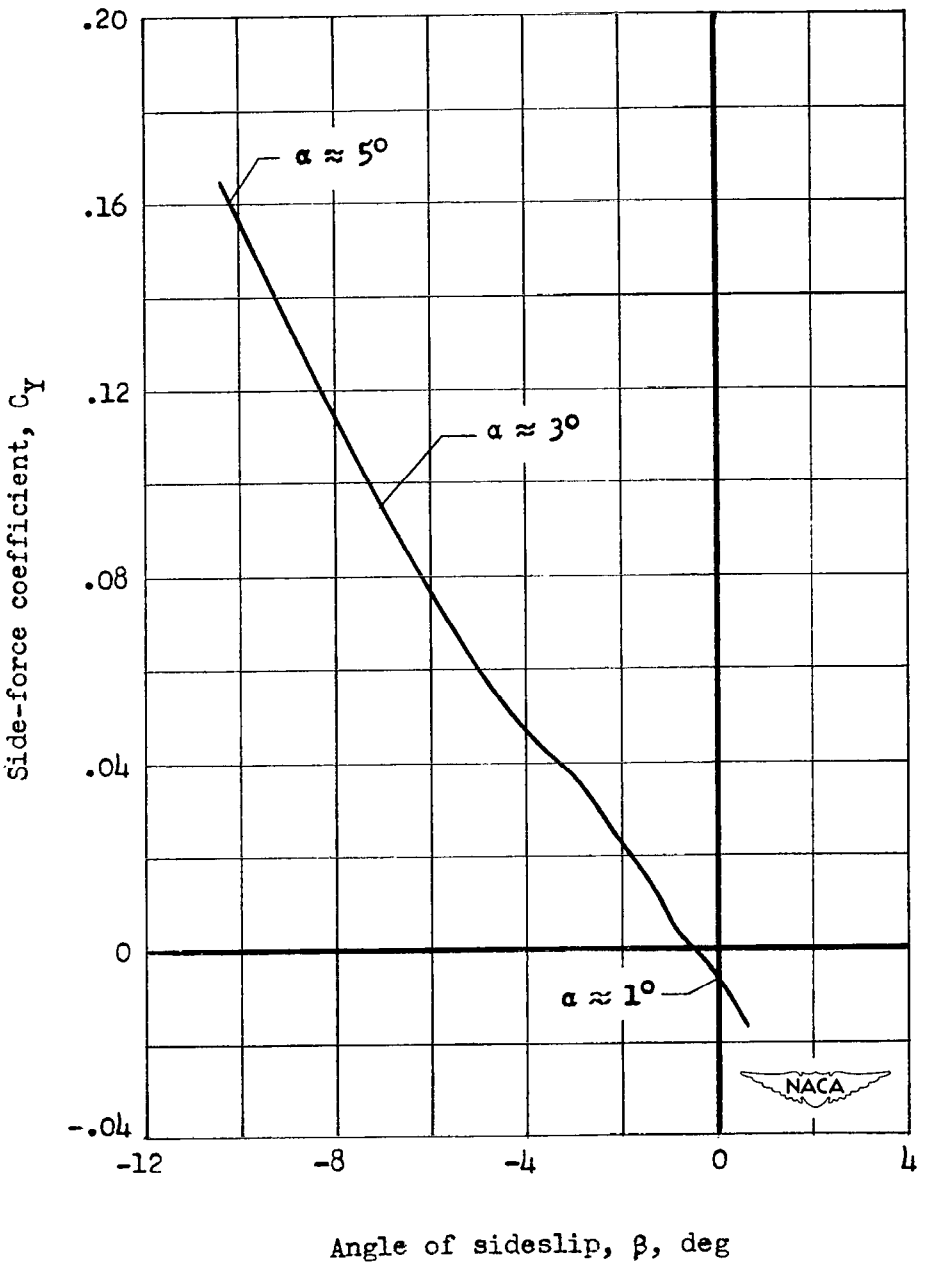

Figure 5.- Variation of side-force coefficient with angle of sideslip from 3.48 to 3.83 seconds at $M \approx 0.88$.

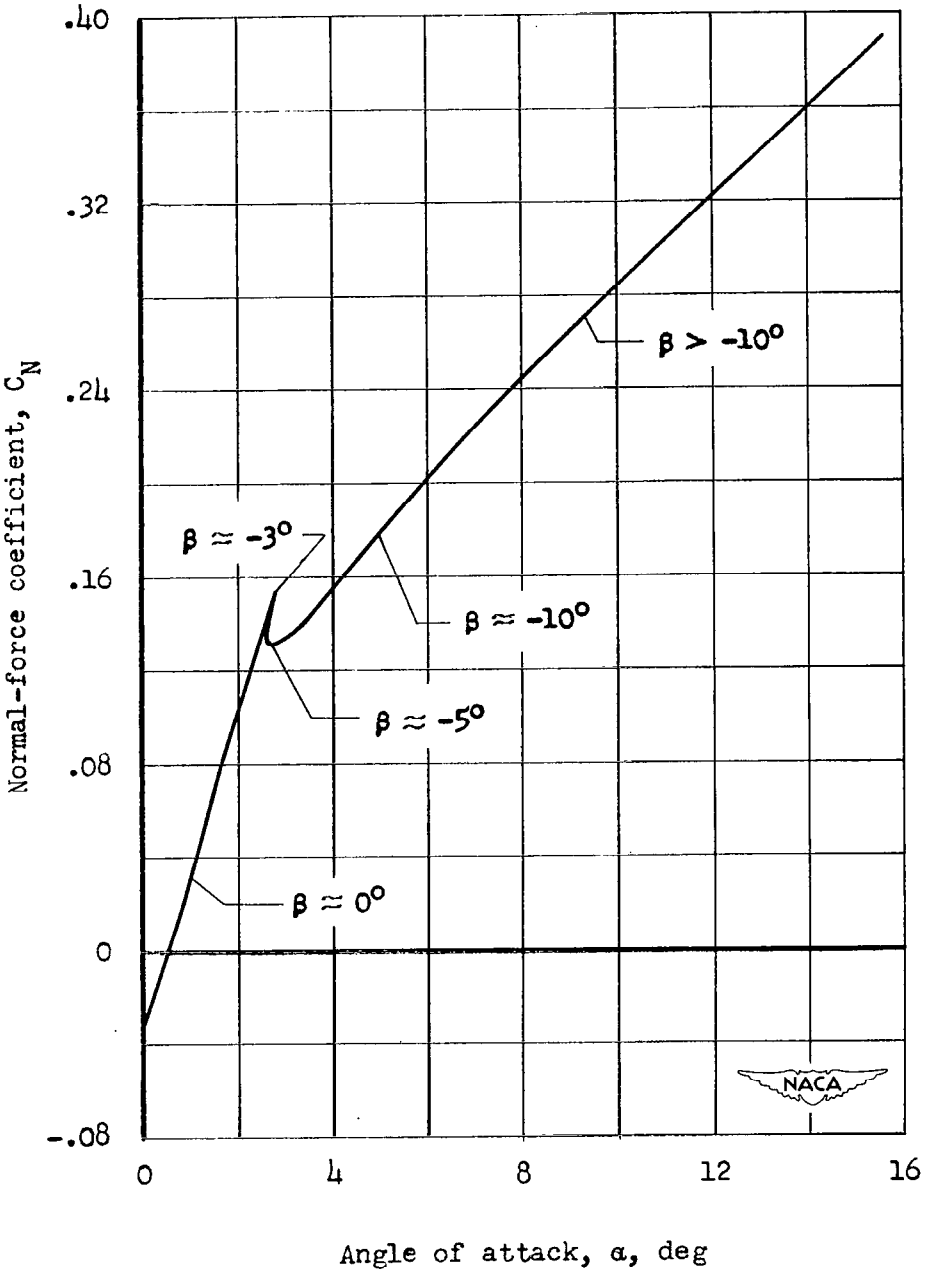

Figure 6.- Variation of normal-force coefficient with angle of attack from 3.50 to 3.95 seconds at $M \approx 0.88$.

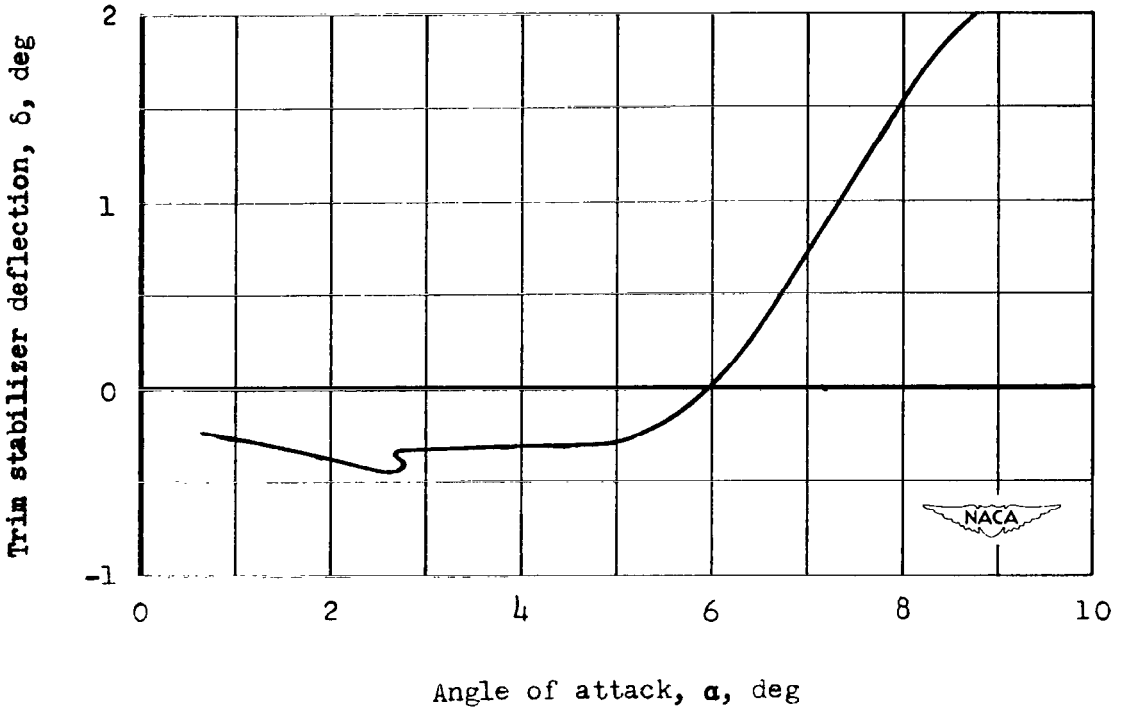

Figure 7.- Variation of trim stabilizer deflection with angle of attack from 3.52 to 3.91 seconds at $M \approx 0.88$ and $\delta_c = 1^\circ$.